Structural calculations for bulk As

L. F. Mattheiss and D. R. Hamann
AT&T Bell Laboratories, Murray Hill, New Jersey 07974-2070

W. Weber
Institut Für Nukleare Festkörperphysik, Kernforschungszentrum Karlsruhe G.m.b.H., Postfach 3640, D-7500 Karlsruhe 1, Federal Republic of Germany

(Received 14 April 1986)

The valence-electron contribution to the total energy of simple-cubic and rhombohedral arsenic has been calculated with use of local-density-functional theory and a scalar-relativistic version of the linear augmented-plane-wave method. The results at normal pressure show that the observed rhombohedral ($A7$) structure is favored energetically over the cubic phase by about 0.07 eV/atom. The calculated values for the lattice parameter ($a=4.084$ Å), rhombohedral angle ($\alpha=55.9°$), and internal displacement parameter ($u=0.2294$) are in excellent agreement ($\sim 0.3\%$, 2%, and 0.8%, respectively) with experiment. The cubic-rhombohedral energy difference, which is due to a Peierls-type mechanism at normal volume, is found to decrease at reduced volumes, leading to a stable high-pressure (~ 190 kbar) cubic phase for $V/V_0 \lesssim 0.8$.

I. INTRODUCTION

A notable property of the group-VA elements and the isoelectronic IV-VI binary compounds is their tendency to crystallize in low-symmetry rhombohedral and orthorhombic structures that are distorted variations of the cubic rocksalt structure.[1,2] A feature that is shared by each of these distorted structures is the presence of double layers of atoms in which each site has three nearest neighbors along nearly orthogonal directions. These structural regularities among the materials with an average valence of five are in marked contrast to the well-known tetrahedral coordination of the group-IVA elements.

Cohen, Falicor, and Golin[1] have advanced simple chemical arguments to explain these differences. In the tetravalent materials, the s^2p^2 configuration of the atom evolves to an sp^3 configuration in the solid, producing hybridized orbitals that are appropriate for the formation of covalent bonds in tetrahedrally coordinated structures. The increase in the s-p energy separation between the group-IVA and group-VA elements is sufficient to minimize these hybridization effects, resulting in a p^3 configuration for the pentavalent materials. Unhybridized p orbits favor bond formation along three orthogonal directions which, in the simplest case, corresponds to the simple-cubic structure. In the covalent limit, one expects the simple-cubic structure to be unstable because of the presence of unsaturated p bonds. The cubic-rhombohedral distortion serves to remove this degeneracy and provides a geometry in which the three nearest-neighbor bonds are both nearly orthogonal and saturated.[2]

The initial efforts to understand the energetics of these noncubic distortions have focussed primarily on the rhombohedral phase of As. They utilized a pseudopotential perturbation-expansion method[3] in combination with an empirical pseudopotential fitted to the As Fermi surface.[4] While the earliest second-order calculations[5] yielded quite reasonable results, the agreement between the calculated and observed geometries was spoiled by the inclusion of third-order terms.[6] Subsequent calculations involving the use of a pseudopotential that was untruncated at large wave vectors[7] and a self-consistent approach[8] were more successful. However, the limited scope of these later studies precluded a complete determination of the equilibrium geometry for rhombohedral As.

Very recently, first principles pseudopotential total-energy methods have been applied in a more comprehensive study of this class of materials. The calculations by Rabe and Joannopoulos[9] have focussed on the two IV-VI compounds SnTe and PbTe. More recently, Needs *et al.*[10] have carried out a similar study of the structural properties of simple-cubic and rhombohedral As.

In this paper, we present the results of an independent study of the structural properties of cubic and rhombohedral As involving the use of a recently developed version of the linear augmented-plane-wave (LAPW) method[11] and local-density-functional theory.[12] The results of this study, which was completed before we learned of the work of Needs, Martin, and Nielsen,[10] provide a useful comparison of total-energy results in a low-symmetry system where the structural-energy differences are of the order of 0.1 eV/atom.

A complete determination of the rhombohedral α-arsenic (or $A7$) structure requires the evaluation of three independent parameters, including the lattice constant a, the rhombohedral angle α, and an internal displacement parameter u. The nature of the $A7$ structure is most easily understood in terms of successive distortions to the simple-cubic structure. The basic distortion is a [111] displacement corresponding to a zone-boundary R-point vibration. This leads to an fcc-type unit cell containing two atoms, similar to that of the rocksalt structure. The R-point phonon can be seen as a dimerization of neighboring (111) planes (internal displacement parameter

$u = 0.25 \pm \Delta u$). This motion accompanies a shear distortion that decreases the rhombohedral angle α between the primitive lattice vectors from their undistorted fcc value, $\alpha = 60°$.

Unlike the pseudopotential approach,[10] the LAPW basis functions are structure dependent so that the calculation of stresses and forces is nontrivial. Consequently, we have adopted a more direct approach to the problem of evaluating the three independent parameters (a, α, and u) of the $A7$ structure. Namely, we have carried out initial calculations in which only the volume (or lattice constant a) was varied, with the rhombohedral angle and internal-displacement parameter fixed at their observed values (α_0 and u_0, respectively). Then, using this calculated minimum-energy volume, subsequent calculations were carried out for discrete values of $\Delta\alpha$ and Δu and a "relaxed" value for the minimum energy was determined by interpolation. The close agreement between the relaxed and unrelaxed energies ($\sim 1 \times 10^{-4}$ hartree/atom) and the calculated and observed[13] values of α ($\sim 2\%$) and u ($\sim 0.8\%$) verifies the accuracy of this approach.

A comparison of the present LAPW valence-energy results for simple cubic and rhombohedral As with the previous results of Needs, Martin, and Nielson[10] reveals qualitative agreement. One discrepancy concerns the normal pressure cubic-rhombohedral structural-energy difference, which is 0.07 and 0.12 eV/atom according to the LAPW and pseudopotential results, respectively. A second difference concerns the stability of the simple-cubic phase at reduced volumes. Contrary to the pseudopotential results, the present LAPW calculations predict that the simple-cubic structure is stable in regard to rhombohedral distortions when $V/V_0 \lesssim 0.8$.

The details of the present LAPW calculations are summarized in Sec. II, including an analysis of the $A7$ crystal structure. The principal results of our investigation are presented in Sec. III. This discussion includes comparisons with previous calculations and experiment in regard to structural as well as one-electron (energy-band, charge-density, and density-of-states) properties. Section IV presents the conclusions that have been derived from this investigation.

II. DETAILS OF THE CALCULATION

A. $A7$ crystal structure

The heavier members of the group-V A column of the Periodic Table (As, Sb, and Bi) share the same α arsenic or $A7$ structure[13] with the space group D_{3d}^5 ($R\bar{3}m$). The primitive unit cell, which is shown in Fig. 1(a), is generated by the rhombohedral lattice vectors,[14]

$$\begin{aligned} \mathbf{t}_1 &= s\hat{\mathbf{i}} + r\hat{\mathbf{k}} , \\ \mathbf{t}_2 &= -(s/2)\hat{\mathbf{i}} + (\sqrt{3}s/2)\hat{\mathbf{j}} + r\hat{\mathbf{k}} , \\ \mathbf{t}_3 &= -(s/2)\hat{\mathbf{i}} - (\sqrt{3}s/2)\hat{\mathbf{j}} + r\hat{\mathbf{k}} . \end{aligned} \tag{1}$$

It is conventional to denote the length of these vectors by a and the angle between them by α, leading to the relations $a^2 = s^2 + r^2$ and $s = (2a/\sqrt{3})\sin\alpha/2$. It is readily shown that these rhombohedral lattice vectors are identical to those for the fcc structure when $\alpha = 60°$ and $r/s = \sqrt{2}$.

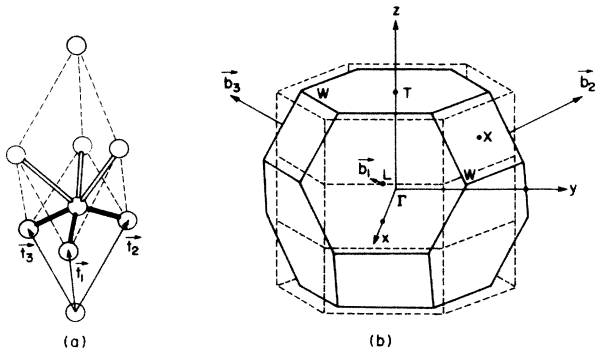

FIG. 1. (a) Primitive unit cell for rhombohedral As. Nearest- and second-neighbor bond directions are indicated by the filled and outlined cylinders respectively. (b) Brillouin zone for the primitive rhombohedral lattice (solid lines) compared with that for a nonprimitive hexagonal cell (dashed lines).

Each primitive cell of the $A7$ structure contains two As atoms. Although the origin is drawn at one of these sites in Fig. 1(a) to illustrate clearly the near-neighbor coordination, it is conventional to choose the origin at the inversion center that is located midway between the closest pair of atoms along the vertical axis. In this case, the atom positions are given by

$$\mathbf{r}_\pm = \pm u(\mathbf{t}_1 + \mathbf{t}_2 + \mathbf{t}_3) = \pm 3ur\hat{\mathbf{k}} . \tag{2}$$

The point-group symmetry about each atomic site is C_{3v}.

The nearest- and second-neighbor bondlengths, which are indicated by the filled and outlined cylinders in Fig. 1(a), are determined by the relations

$$\begin{aligned} d_{1\mathrm{NN}} &= [s^2 + r^2(1-6u)^2]^{1/2} , \\ d_{2\mathrm{NN}} &= [s^2 + r^2(2-6u)^2]^{1/2} . \end{aligned} \tag{3}$$

These are equal for $u = 1/4$. It can be shown that, aside from a difference in orientation, an identical structure is obtained for $u = 0.25 \pm \Delta u$. Normally, values of $u < 0.25$ are reported.

Instead of considering a primitive rhombohedral cell, it is common to treat a nonprimitive hexagonal cell with lattice parameters $a_h = \sqrt{3}s$ and $c_h = 3r$. This yields a cell containing six atoms with a volume that is three times larger than that of the primitive rhombohedral cell, $V = \frac{1}{2}3\sqrt{3}s^2 r$.

The primitive reciprocal lattice vectors for the rhombohedral structure also form a rhombohedral lattice and are given by

$$\begin{aligned} \mathbf{b}_1 &= 2\pi[2/(3s)\hat{\mathbf{i}} + 1/(3r)\hat{\mathbf{k}}] , \\ \mathbf{b}_2 &= 2\pi[-1/(3s)\hat{\mathbf{i}} + \sqrt{3}/(3s)\hat{\mathbf{j}} + 1/(3r)\hat{\mathbf{k}}] , \\ \mathbf{b}_3 &= 2\pi[-1/(3s)\hat{\mathbf{i}} - \sqrt{3}/(3s)\hat{\mathbf{j}} + 1/(3r)\hat{\mathbf{k}}] . \end{aligned} \tag{4}$$

Using the observed[13] structural parameters for As, these vectors produce the Brillouin zone whose shape is illus-

trated by the solid lines in Fig. 1(b). This primitive rhombohedral zone has the same volume as the three nonprimitive hexagonal zones that are indicated by the dashed lines.

B. Structural energies

A detailed description of the methods that have been applied in the present LAPW study of simple-cubic and rhombohedral As has been published recently.[11] In the present section, we highlight those aspects of the method that are important in the present study as well as provide values for various LAPW parameters and their cutoffs.

The present LAPW implementation is similar to the pseudopotential method in that it incorporates a rigid-core approximation. This allows the calculation of the valence-electron contribution to the total energy rather than the total energy itself. The core charge density and potential are derived from an atomic calculation involving an assumed $4s^2 4p^3$ valence-electron configuration. Both the LAPW and atom calculations have been carried out using a scalar-relativistic approximation so that all relativistic effects except spin-orbit coupling are included. Exchange-correlation effects are introduced using the Wigner interpolation formula.[15]

Various computational parameters have been fixed throughout the calculations in order to provide structural-energy differences that are better converged than the absolute energies themselves. The muffin-tin radius has been set at the value $R \approx 2.167$ a.u., which corresponds to about 45% of the nearest-neighbor distance for the observed rhombohedral structural parameters.[13] The LAPW basis-set size has been determined using a plane-wave kinetic-energy cutoff of 4.5 hartree. This provides a volume-dependent basis size that varies from 50—70 LAPW's per atom over the volume range (105—157.5 a.u./atom) of the present calculations. The corresponding cutoff for the Fourier-series expansion of the charge density and potential in the interstitial region was set at 50 hartree (corresponding to about 2500 plane waves/atom).

The spherical-harmonic expansion of the LAPW wave functions within the muffin-tin spheres included terms up to $l_{\max}=8$. The corresponding lattice-harmonic expansion of the nonspherical contributions to the charge density and potential within the spheres surrounding each atomic site has included all terms through $l=6$. In the case of $A7$ geometry where the site symmetry is C_{3v}, this corresponds to a total of 12 terms in this expansion.

Special care has been taken in regard to the Brillouin-zone sampling procedures. In all cases, the sampling was carried out using a uniform mesh of points in the irreducible wedge of the zone.[16] The meshes were chosen so as to provide the same number of points in the full Brillouin zone for both the $A7$ and simple-cubic structures. (For such considerations, it is appropriate to regard the simple-cubic structure in terms of rocksalt lattice with two atoms per cell and an fcc-type Brillouin zone.)

The simple-cubic and rhombohedral mesh points were generated in such a way that a one-to-one relationship was maintained between points in the full Brillouin zone. Starting from an off-set uniformly distributed simple-cubic mesh, the corresponding rhombohedrally distorted mesh of **k** points was generated, taking into account the [111] shear distortion as well as the reduced point-group symmetry of the $A7$ structure.

For each geometry, the self-consistent calculations were carried out for four iterations using 256 **k** points in the entire Brillouin zone. For the simple-cubic and $A7$ calculations, these corresponded to 20 and 34 **k** points in the irreducible wedge of the zone. After four iterations, the average root-mean-squared deviation between the final input and output potentials was consistently less than 10^{-4} hartree. The change in the calculated valence energy between the third and fourth iterations was less than 10^{-5} hartree/atom.

To avoid possible instabilities during the iterative self-consistent process, populations have been smeared using a Fermi function with a finite temperature, $T=0.001$ hartree. This increases the calculated energy by an amount $\pi^2 T^2 N(E_F)/6$ over the zero-temperature limit, where $N(E_F)$ is the density of states at the Fermi energy E_F. Using density-of-states results that are presented below, these shifts are found to be comparable to the convergence errors [$\sim(1-2)\times 10^{-5}$ hartree/atom] in the self-consistency procedure.

At this point, a final iteration was carried out in which the Brillouin-zone sample was increased from 256 to 864 **k** points. This improved sampling produced changes in the calculated valence energies that were less than 5×10^{-4} hartree/atom with minimal effect on the self-consistency criterion ($\sim 10^{-4}$ hartree). These final results are those presented and discussed in the following section.

III. RESULTS AND DISCUSSION

The first-stage results of the present LAPW structural calculations for bulk As are shown in Fig. 2. Here, the valence-electron contribution to the total energy of As is

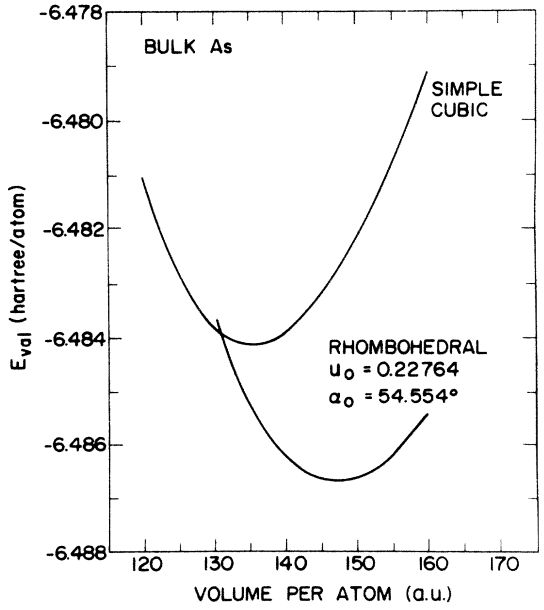

FIG. 2. Calculated LAPW valence energy as a function of volume for the simple-cubic and rhombohedral structures.

plotted as a function of volume for the simple-cubic and rhombohedral structures. The curves are obtained from cubic (quartic) fits to the calculated rhombohedral (simple-cubic) energies at equally spaced volumes between 135 and 157.5 a.u./atom (127.5 and 157.5 a.u./atom). The results of a subsequent simple-cubic calculation at $V=120$ a.u./atom agreed with the quartic extrapolation to within 10^{-6} hartree/atom.

As indicated, the rhombohedral results in Fig. 2 have been evaluated for a fixed geometry in which the rhombohedral angle α and the internal displacement are set at their observed values, α_0 and u_0, respectively. The curves show that, even for this unrelaxed geometry, the energy of the rhombohedral phase is lower than that of the simple-cubic structure by about 0.0026 hartree/atom ($\sim$0.07 eV/atom). It is estimated below that the subsequent relaxation of α and u will increase this structural energy difference by $\sim 1\times 10^{-4}$ hartree/atom.

The calculated minimum-energy volume for the rhombohedral phase, $V_r=147.1$ a.u./atom, is in excellent ($\sim$2%) agreement with the observed value,[13] 143.8 a.u./atom. It is about 9% larger than that calculated for the simple-cubic structure (135.4 a.u./atom).

In order to determine the effect of relaxing α and u on the calculated rhombohedral valence energy, additional calculations have been carried out at fixed volume V_r in which both parameters have been systematically varied. In particular, these calculations have considered the 20 geometries that result from four choices of α (60°, 57.25°, 54.5°, 51.75°) and five u (0.25, 0.238, 0.23, 0.226, 0.214) values, respectively.

The results derived from these calculations are plotted as contours of constant valence energy in Fig. 3. The contour values denote energy differences (in units of 10^{-3} hartree/atom) relative to the simple-cubic results at the origin ($\alpha=60°$, $u=0.25$) where $E_{\rm val}=-6.482\,81$ hartree/atom. The contours have been calculated using interpolated intermediate values (i.e., a series of polynomial fits to the calculated energies, first as a function of α, then as a function of u), taking into account the symmetry about $u=\frac{1}{4}$.

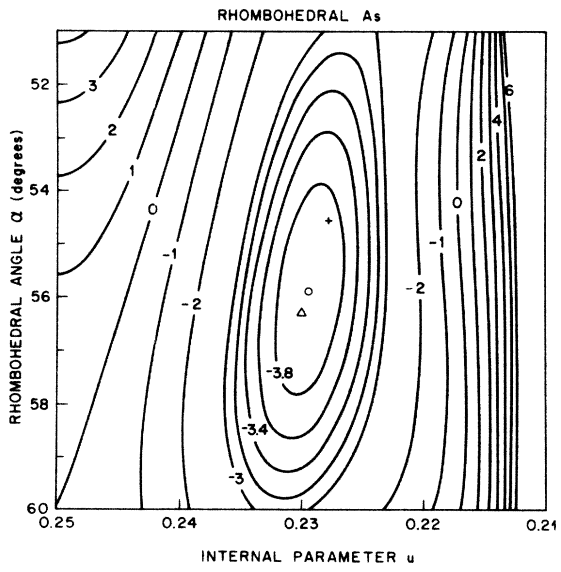

FIG. 3. Calculated dependence of the LAPW valence-energy results on α and u at fixed volume ($V_r=147.1$ a.u./atom). Contour values (in units of 10^{-3} hartree/atom) are plotted relative to simple-cubic valence energy. The open circle, triangle, and cross denote calculated LAPW, pseudopotential (Ref. 10), observed (Ref. 13) structural parameters, respectively.

The constant-energy contours are nearly elliptical in shape in the vicinity of the energy minimum $E_{\rm min}=-0.003\,98$ hartree/atom. The position of this minimum is indicated by the open circle. The corresponding values of the structural parameters are $\alpha=55.9°$ and $u=0.2294$. The cross indicates the observed combination of parameters α_0 and u_0. The interpolated energy at this point is $\sim 1\times 10^{-4}$ hartree/atom above $E_{\rm min}$. It agrees with the calculated LAPW energy to $\sim 10^{-5}$ hartree/atom. The triangle represents the corresponding pseudopotential results of Needs, Martin, and Nielsen[10] which are discussed below.

The ratio of the major-to-minor axes of the lowest-energy ellipse in Fig. 3 is about 3.5:1. Its orientation relative to the coordinate axes shows that the valence energy of rhombohedral As is more sensitive to variations in u than in α. This is consistent with the fact that the calculated value of u is in better agreement with experiment ($\sim$0.8%) than the corresponding agreement in α ($\sim$2%).

Presumably, the shape and orientation of these elliptical contours in Fig. 3 are related to the fact that, at constant volume, the nearest-neighbor distance $d_{\rm 1NN}$ is more strongly dependent on u than α. For example, near the calculated minimum, a 1% variation in u produces a 1% change in $d_{\rm 1NN}$. On the other hand, a corresponding variation in α changes $d_{\rm 1NN}$ by only 0.1%.

One can determine the frequency of the zone-center Γ_1 optic mode from the curvature of $E_{\rm val}$ versus u at the calculated minimum in Fig. 3. The calculated value for this frequency, $\sim$220 cm^{-1}, is in reasonable agreement with the measured[17] value of 254 cm^{-1}, given the coarse mesh of atomic displacements that are involved in this frozen-phonon calculation and the fact that interpolated energies are used to evaluate the curvature. By comparison, the pseudopotential calculations[10] provide a frequency of $\sim$250 cm^{-1} that is in excellent agreement with experiment.

We present in Fig. 4 a detailed comparison between the LAPW valence-energy results for cubic and rhombohedral As and the pseudopotential results of Needs, Martin, and Nielsen.[10] In this plot, the pseudopotential energies have been lowered by $\sim$0.1141 hartree/atom in order to equalize the minimum simple-cubic energies of the two calculations. It is emphasized that only the simple-cubic results in Fig. 4 are directly comparable. The corresponding results for the $A7$ structure involve different geometries: one that is fixed (LAPW) and one that is relaxed (pseudopotential).

The results of the pseudopotential calculations for simple-cubic As predict an energy minimum at a volume which is about 3% smaller than the corresponding LAPW result. In addition, the curvature near the pseudopotential minimum is about 20% greater than that of the corre-

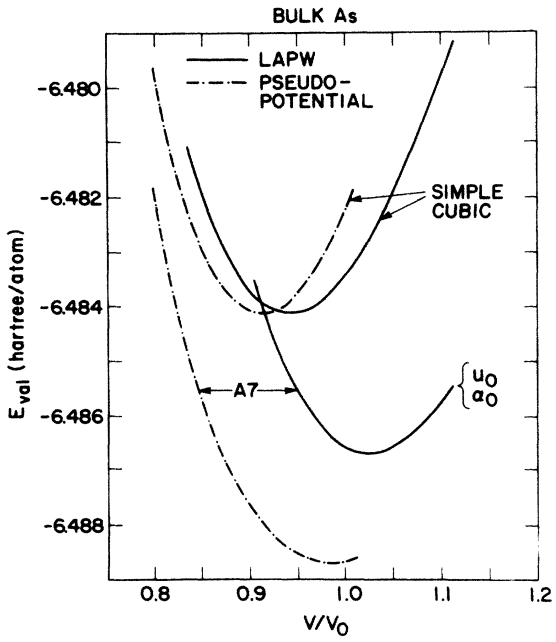

FIG. 4. Comparison of LAPW and pseudopotential results (Ref. 10) as a function of volume for simple-cubic and rhombohedral As, where $V_0=143.8$ a.u./atom is the observed volume at atmospheric pressure. The pseudopotential energies have been lowered by -0.114 hartree/atom to facilitate this comparison.

sponding LAPW curve. The LAPW and pseudopotential values for the lattice parameter and bulk modulus of simple-cubic As are listed in the upper portion of Table I.

Larger differences are exhibited by the corresponding results for the $A7$ phase in Fig. 4. Some of these differences (such as the reduced curvature of the pseudopotential results near the minimum) are expected on the basis of the relaxed pseudopotential geometry. For example, the optimization of α and u as a function of volume will lead to a lowering of the calculated valence energies, thereby decreasing the overall curvature of the LAPW $A7$ results near the minimum. However, it is clear from Fig. 4 that these changes, which amount to $\sim 10^{-4}$ hartree/atom near the LAPW $A7$ minimum, will not alter the result that the pseudopotential calculations predict a simple-cubic—to—$A7$ structural-energy difference, ~ 0.12 eV/atom, that is significantly larger than the LAPW result, ~ 0.07 eV/atom.

TABLE I. Comparison of the calculated and observed structural properties for simple-cubic and rhombohedral As. ΔE_{val} is the cubic-rhombohedral energy difference while E_{coh} is the cohesive energy.

Structure/Property	Pseudo[a]	LAPW[b]	Experiment
	Cubic		
a (Å)	2.687	2.717	
B (Mbar)	1.04	0.87	
	Cubic rhombohedral		
ΔE_{val} (eV/atom)	0.124	0.069	
	Rhombohedral		
a (Å)	4.017	4.084	4.1018[c]
α (deg)	56.28	55.9	54.554[c]
u	0.230	0.2294	0.227 64[c]
E_{coh} (eV/atom)		3.78	2.96[d]
B (Mbar)	0.43	(0.77)[e]	0.383[f]

[a] Reference 10.
[b] Present work.
[c] Reference 13.
[d] Reference 18.
[e] Calculated for fixed α and u values of Ref. 13.
[f] Reference 19.

A factor that may be partially responsible for the 3% discrepancy in volume between the LAPW and pseudopotential simple-cubic results in Fig. 4 is the limited Brillouin-zone sampling involved in the pseudopotential calculations. A reduction in the LAPW full-zone sample from 1728 to 512 **k** points (corresponding to 56 and 20 points, respectively, in the irreducible wedge) shifts the LAPW simple-cubic minimum to a volume that is about 1% smaller than that shown in Fig. 4. However, these effects cannot account for the discrepancy between the calculated cubic-$A7$ structural-energy differences. In particular, the analogous LAPW $A7$ valence-energy results with reduced-zone sampling have their minimum shifted to a slightly larger ($\sim 0.2\%$) volume while maintaining (to within 0.001 eV) the same 0.07-eV cubic-$A7$ structural-energy difference.

The linear-compressibility results of Morosin and Schirber[19] allow one to understand the reduced curvature of the pseudopotential $A7$ energy curve near its minimum in comparison with the LAPW results in terms of relaxation effects. Denoting the linear compressibilities along directions parallel and perpendicular to the trigonal axis by k_c and k_a, respectively, one can rewrite the volume compressibility $k_v=2k_a+k_c$ as a sum of two contributions: one involving a fixed rhombohedral angle ($3k_a$); and a second as a variable-angle contribution (k_c-k_a). According to the Morosin-Schirber results,[19] the latter represents about 87% of the total volume compressibility of As. An analysis[20] of earlier data for As provides a somewhat smaller ($\sim 78\%$) estimate of this contribution.

A summary of the calculated and observed $A7$ structural properties is contained in the lower portion of Table I. As indicated, the LAPW structural parameters are generally in slightly better agreement with experiment than the corresponding pseudopotential results. One exception, of course, is the bulk modulus, which is overestimated in the LAPW calculation because of the omission of relaxation effects.

The calculated value for the cohesive energy in Table I is about 0.8 eV/atom larger than the observed value. This overestimate is consistent with previous calculations[11] for the group-VIB elements Cr, Mo, and W. The lowest energy for the As atom, $E_{atom}=-6.3477$ hartree, has been obtained by means of a spin-polarized calculation for a valence-electron configuration of $4s_\uparrow 4s_\downarrow 4p_\uparrow^3$. The calculation assumes a rigid core which is identical to that used in the bulk calculations. The scaling prescription of von Barth and Hedin[21] has been applied to generalize the Wigner interpolation formula[15] to the spin-polarized situ-

ation. This calculated atomic valence energy is in reasonable accord with the experimental value (-6.234 hartree) that is obtained by summing the first five experimental ionization energies.[22]

An interesting issue that has not yet been resolved experimentally concerns the stability of simple-cubic As phase at compressed volumes. Intuitively, one expects that the application of hydrostatic pressure to the $A7$ crystal structure of Fig. 1(a) would tend to equalize the near-neighbor bond distances and increase the rhombohedral angle, leading eventually to a more close-packed simple-cubic phase at reduced volumes. This expectation is quite reasonable in the case of As since a high-pressure simple-cubic phase has been observed in the neighboring group-V A elements P (Refs. 23 and 24) and Sb (Ref. 25) at pressures of 110 and 70 kbar, respectively.

The familiar theoretical approach to identifying a high-pressure structural phase transition is to attempt a common-tangent construction between energy-volume curves like those in Fig. 2. In the present case, however, this is incorrect. The simple-cubic phase can be continuously deformed into the $A7$ structure, so that an $A7$ curve with α and u optimized at each volume could at most merge with the cubic curve, not cross it. The pseudopotential curves reproduced in Fig. 4 do not merge, and the authors infer that they remain separated at smaller volumes than those for which calculations were performed.[10]

An alternative approach is to study the stability of the simple-cubic phase with respect to small changes of α and u from their cubic values. We find it to be unstable with respect to a u-type distortion (R-point phonon) at larger volumes, but to become stable for $V<115$ a.u./atom ($V/V_0<0.8$). Detailed results illustrating the cross over are shown in Fig. 5. The cross over implies that we would find our optimized $A7$ curve merging with the cubic energy-volume curve with a common tangent at $V/V_0\approx 0.8$. From the slope at this point, we estimate that the $A7$-cubic transition should occur at ~ 190 kbar. These results are at variance with those of the pseudopotential study. In addition to the noncrossing of their curves, those authors found the cubic phase to remain unstable down to the smallest volume examined.[10] They find it to be stable with respect to α-type distortions (rhombohedral shears) at all volumes, as do we.

Our expected trend toward a stable simple-cubic As phase at high pressures is consistent with the observed pressure dependence of α and u. In addition to the linear compressibilities, Morosin and Schirber[19] have measured the variation of u with pressure. According to their results, both α and u increase with pressure towards their simple-cubic values at rates given by $d(\ln\alpha)/dP\approx 1.8$ Mbar^{-1} and $d(\ln u)/dP\approx 1.2$ Mbar^{-1}, respectively. McWhan[26] has combined these results with additional high-pressure data to show that the As rhombohedral angle α approaches 60° at a reduced volume $V/V_0\approx 0.8$, in surprisingly good agreement with our result.

In their study of superconductivity at high pressures in As, Berman and Brandt[27] have observed a jump in T_c at pressures near 140 kbar which may be related to the proximity of an $A7$—simple-cubic structural transformation.

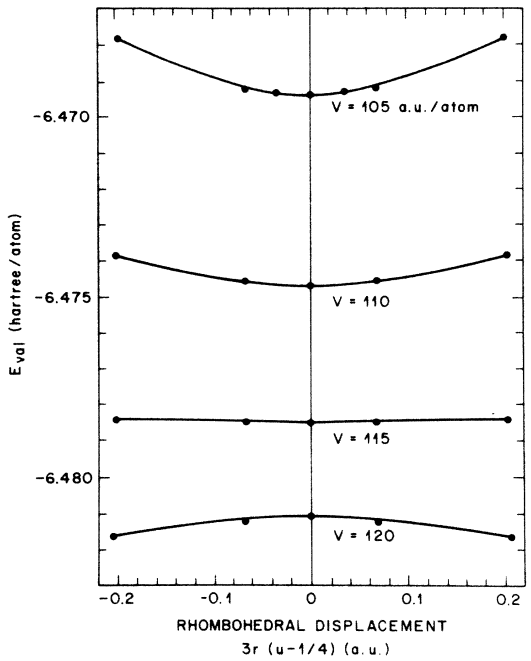

FIG. 5. Calculated LAPW valence energies (solid circles) versus rhombohedral displacements near the crossover volume $V\approx 115$ a.u./atom below which the simple-cubic phase is stable. The solid lines are parabolas determined by the central and outermost energy values.

The application of uniaxial pressures in this range have been reported[28] to yield a complicated metastable tetragonal structure that persists after the pressure is released. Therefore, it is possible that a transition to a more close-packed As phase may occur before the $A7$-cubic transition is reached.

In order to obtain a better understanding of the energetics of the cubic-rhombohedral distortion, it is useful to examine the band properties of the two phases. The LAPW band structure for simple-cubic As at its minimum-energy volume (135.4 a.u./atom) is shown in Fig. 6. The band profiles exhibit characteristic tight-binding features, including a single low-lying band with predominantly $4s$

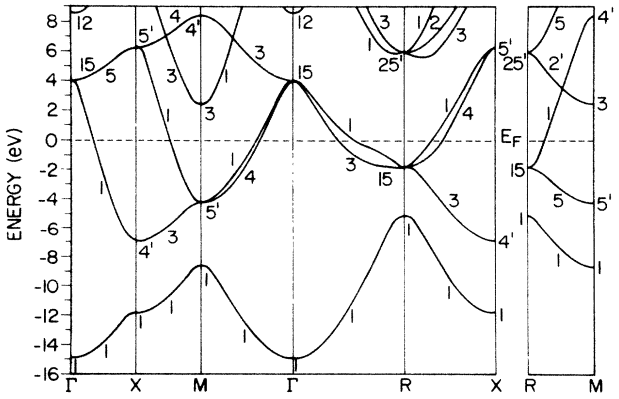

FIG. 6. LAPW band structure for simple-cubic As at $V_c=135.4$ a.u.

character as well as a half-filled $4p$ band that is approximately centered about E_F. A subband of the higher-energy $4d$ manifold overlaps the unoccupied $4p$ bands near M.

Using a simple tight-binding model (involving nearest-neighbor interactions and a two-center approximation), Weber has shown[29] that a half-filled simple-cubic p band leads to electron and hole Fermi-surface sheets that nest perfectly when the R point is folded back into the zone center. This suggests that the cubic-$A7$ distortion is driven by a Peierls-type instability involving an R-point phonon. A plot of the folded simple-cubic bands for As, which is shown in Fig. 7(a), demonstrates that the main features of this nesting are preserved in the present LAPW results. The effect of the rhombohedral distortion on these folded simple-cubic bands is shown in Fig. 7(b). These rhombohedral results are derived from the minimum-energy geometry of Fig. 2 ($V_r = 147.1$ a.u./atom). As expected, the reduced symmetry of the rhombohedral phase is found to eliminate many of the band crossings near E_F as well as the accidental degeneracies that occur throughout the hexagonal faces of the fcc equivalent to the rhombohedral Brillouin zone of Fig. 1(b).

A comparison of the LAPW results in Fig. 7 with a similar plot of the corresponding pseudopotential results of Needs, Martin, and Nielsen[10] indicates excellent overall agreement. Small differences in the cubic results (~ 0.5 eV) are attributed to the larger volume (145.2 a.u./atom) in the pseudopotential calculation. Equally good agreement is obtained in regard to the self-consistent pseudopotential results of Tokailin *et al.*[30] which have been compared in detail with the companion angle-resolved photoemission results. Unlike the early results,[4] each of the present calculations predicts a Fermi surface involving a single electron pocket at the L point, in accord with experiment.[31]

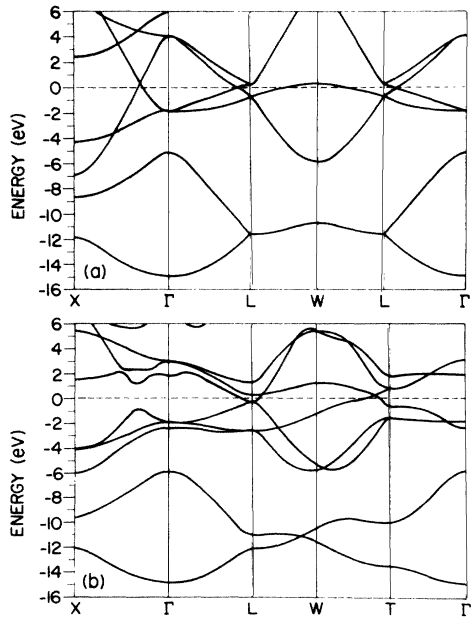

FIG. 7. Comparison of the folded simple-cubic As band structure (a) with that for rhombohedral As (b), plotted along analogous directions in the corresponding Brillouin zones.

The stabilizing effect of the rhombohedral distortion is seen more directly in a comparison of the simple-cubic and rhombohedral density-of-states curves which are shown in Fig. 8. The cubic results have been calculated using the tetrahedral method,[32] with a total of 84 **k** points in the irreducible wedge of the Brillouin zone (1728 points in the full zone). The corresponding rhombohedral calculation has utilized a root-sampling procedure involving 216 (2048) points in the irreducible wedge (full zone). Both curves have been smoothed with a Gaussian having a full width at half maximum of 0.5 eV.

A comparison of these density-of-states results shows that the principal effect of the rhombohedral distortion is to split the simple-cubic peaks arising from the $4s$ and $4p$ bands in a nearly symmetric manner. The splitting of the $4s$ peak, which is about 11.5 eV below E_F, has minimal effect on the stability of the rhombohedral phase. On the other hand, the corresponding splitting of the broad $4p$ peak that is centered about E_F is seen to cause a significant reduction in the average band energy of the states just below E_F.

Because the nearest-neighbor coordination in the rhombohedral phase is reduced from six to three nearest neighbors, one expects an increase in the strength of the $A7$ intralayer bonds in comparison with the corresponding simple-cubic results. This effect is illustrated in the charge-density results shown in Fig. 9 where we compare the charge-density contours in a simple-cubic (110) plane with those in an analogous plane of the rhombohedral structure. It is found that the combined effects of the shear distortion ($\Delta\alpha$) and the dimerization (Δu) is to increase the bond charge density from about 0.05 to 0.07 electrons/a.u.^{3} along the three nearest-neighbor directions and to reduce it by a factor of 2 along second-neighbor directions.

In general, the present LAPW $A7$ charge-density results are in good qualitative agreement with the

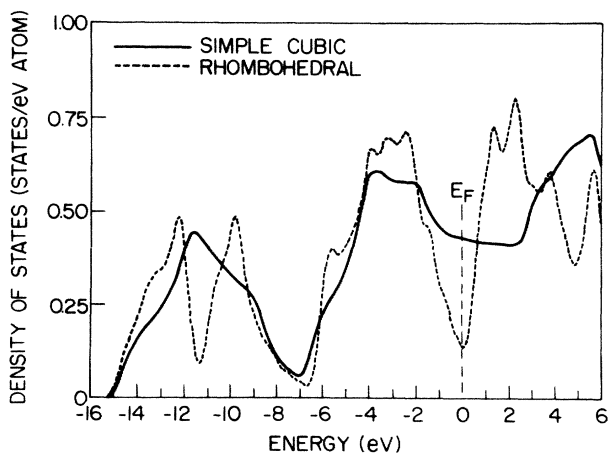

FIG. 8. Valence-band density-of-states curves for simple-cubic and rhombohedral As.

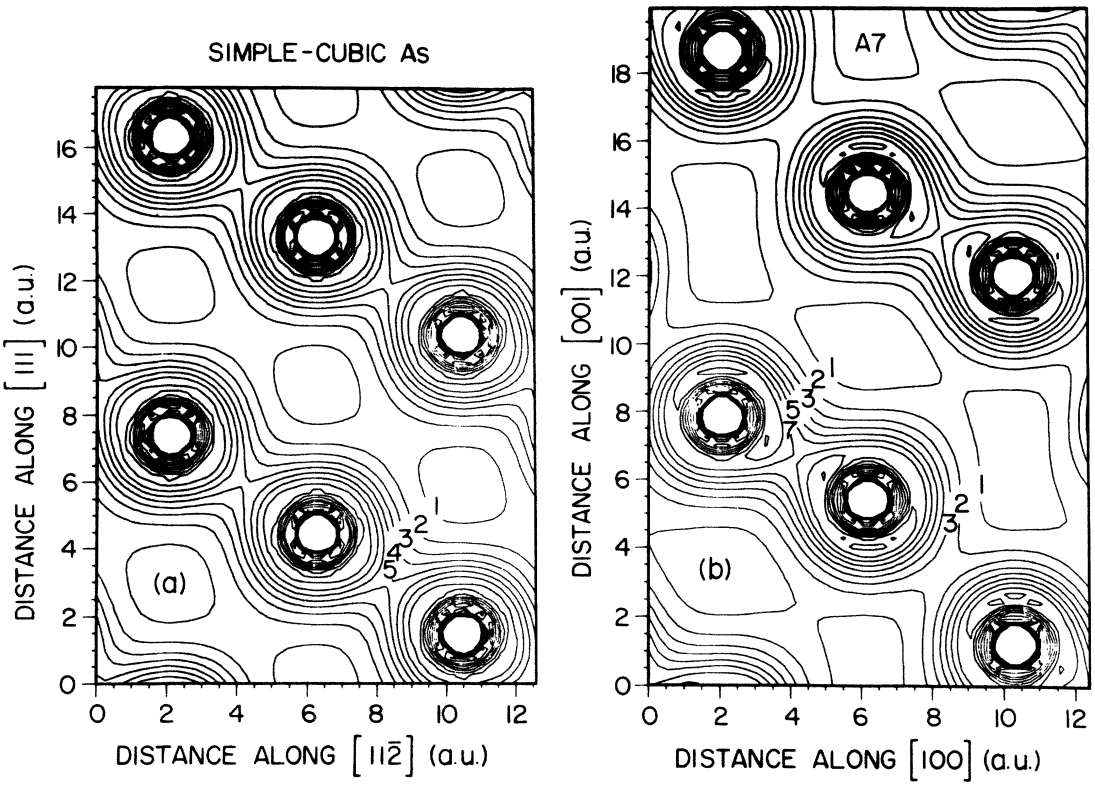

FIG. 9. Calculated valence-electron charge-density results for (a) simple-cubic and (b) rhombohedral As plotted in a (110) cubic plane and its rhombohedral equivalent. Contour intervals are in units of 10^{-2} electrons/a.u.^{3}.

orthogonalized-plane-wave (OPW) results of Golin and Stocco.[33] However, these OPW results exhibit slightly higher ($\sim$0.01 electrons/a.u.^{3}) charge densities along the nearest-neighbor bond directions.

IV. CONCLUSIONS

We have applied the LAPW method to calculate the valence-electron contribution to the total energy of simple-cubic and rhombohedral As. We find that the energy of the rhombohedral structure is about 0.07 eV/atom lower than that of simple-cubic As. The calculated structural parameters are in excellent (1—2%) agreement with the observed values.

The present LAPW results are in reasonable overall agreement with those obtained in a recent pseudopotential study[10] of this system. One discrepancy between these two calculations concerns the predicted cubic-$A7$ structural-energy difference, which is $\sim$80% larger according to the pseudopotential results. A second difference involves the stability of the simple-cubic phase at reduced volumes. Contrary to the pseudopotential results, the LAPW calculations show that the simple-cubic phase of As is stable with respect to rhombohedral distortions at volumes below 115 a.u./atom.

ACKNOWLEDGMENTS

We are pleased to acknowledge useful conversations with D. B. McWhan and J. E. Schirber on this subject, especially in regard to the interpretation of their pressure measurements. We are grateful to R. M. Martin for providing a report on Ref. 10 prior to publication.

[1]M. H. Cohen, L. M. Falicov, and S. Golin, IBM J. Res. Dev. **8**, 215 (1964).

[2]P. B. Littlewood, J. Phys. C **13**, 4855 (1980); **13**, 4875 (1980).

[3]V. Heine and D. Weaire, in *Solid State Physics,* edited by H. Ehrenreich, F. Seitz, and D. Turnbull (Academic, New York, 1970), Vol. 24.

[4]P. J. Lin and L. M. Falicov, Phys. Rev. **141**, 562 (1966); **142**, 441 (1966).

[5]D. Weaire and A. R. Williams, in *The Physics of Semimetals and Narrow Gap Semiconductors,* edited by D. L. Carter and R. T. Bate (Pergamon, New York, 1971), p. 35.

[6]Y. Abe, I. Ohkoshi, and A. Morita, J. Phys. Soc. Jpn. **42**, 504 (1977).

[7]A. Morita, I. Ohkoshi, and Y. Abe, J. Phys. Soc. Jpn. **43**, 1610 (1977).

[8]K. Shindo, J. Phys. Soc. Jpn. **47**, 547 (1979).

[9]K. M. Rabe and J. D. Joannopoulos, Phys. Rev. B **32**, 2302 (1985).

[10]R. J. Needs, R. M. Martin, and O. H. Nielsen, Phys. Rev. B **33**, 3778 (1986).

[11]L. F. Mattheiss and D. R. Hamann, Phys. Rev. B **33**, 823 (1986).

[12]P. Hohenberg and W. Kohn, Phys. Rev. **136**, B864 (1964); W. Kohn and L. J. Sham, *ibid.* **140**, A1133 (1965).
[13]D. Schiferl and C. S. Barrett, J. Appl. Cryst. **2**, 30 (1969).
[14]J. C. Slater, *Quantum Theory of Molecules and Solids* (McGraw-Hill, New York, 1965), Vol. 2.
[15]E. Wigner, Phys. Rev. **46**, 1002 (1934).
[16]H. J. Monkhorst and J. D. Pack, Phys. Rev. B **13**, 5188 (1976).
[17]W. Richter, T. Fjeldly, J. Renucci, and M. Cardona, in *Proceedings of the International Conference on Lattice Dynamics,* edited by M. Balkanski (Flammarion, Paris, 1978), p. 104.
[18]C. Kittel, *Introduction to Solid State Physics,* 5th ed. (Wiley, New York, 1976).
[19]B. Morosin and J. E. Schirber, Solid State Commun. **10**, 249 (1972).
[20]F. Birch, in *Handbook of Physical Constants,* edited by S. P. Clark, Jr. (Geological Society of America, New York, 1966), p. 97.
[21]U. von Barth and L. Hedin, J. Phys. C **5**, 1629 (1972).
[22]*CRC Handbook of Chemistry and Physics,* 65th ed., edited by R. C. Weast (CRC Press, Boca Raton, 1984).
[23]J. C. Jamieson, Science **139**, 1291 (1963).
[24]J. Wittig and B. T. Matthias, Science **160**, 994 (1968).
[25]L. F. Vereshchagin and S. S. Kabalkina, Zh. Eksp. Teor. Fiz. **47**, 414 (1964) [Sov. Phys.—JETP **20**, 274 (1965)].
[26]D. B. McWhan, Science **176**, 751 (1972).
[27]I. V. Berman and N. B. Brandt, Pis'ma Zh. Eksp Teor. Fiz. **10**, 88 (1969) [JETP Lett. **10**, 55 (1969)].
[28]M. T. Duggin, J. Phys. Chem. Solids **33**, 1267 (1972).
[29]W. Weber (unpublished).
[30]H. Tokailin, T. Takahashi, T. Sagawa, and K. Shindo, Phys. Rev. B **30**, 1765 (1984).
[31]M. G. Priestley, L. R. Windmiller, J. B. Ketterson, and Y. Eckstein, Phys. Rev. **154**, 671 (1967); J. Vanderkooy and W. R. Datars, *ibid.* **156**, 671 (1967).
[32]O. Jepsen and O. K. Andersen, Solid State Commun. **9**, 1763 (1971); G. Lehmann and M. Taut, Phys. Status Solidi B **54**, 469 (1972).
[33]S. Golin and J. A. Stocco, Phys. Rev. B **1**, 390 (1970).